

Numerical analysis of rudder effects upon ducted propeller units

Alejandro Caldas¹, Marcos Meis¹, Adrián Sarasquete¹

¹Vicus Desarrollos Tecnológicos (VICUSdt), Vigo, Spain

ABSTRACT

It is a well known fact that the use of ducted propellers is a good option for those applications that need high thrust values at low speed. Because of its particular working conditions this is the case of trawlers which velocities when trawling are between 3 and 5 kts. Beyond this, it is of particular interest the effect that steering elements have on two aspects; the effect upon propulsive factors and the manoeuvrability capability.

In the present paper a study of the effects upon propulsive factors and the manoeuvrability by different rudder configurations and shapes have been carried out. There are several options; nozzle-propeller rudder, three rudder arrangements, one rudder arrangements, flow adapted rudders, etc.

The calculations have been carried out in two different phases; in the first one the calculations were carried out in an uniform flow field for the complete system: ducted propeller- rudder/rudders. And for the second one a typical trawler wake field was employed. For both phases the effect of the rudder on the energy efficiency and also the manoeuvrability capabilities of each system were studied. All the calculations have been carried out using commercial CFD code STAR-CCM+.

Keywords

Ducted propeller, Rudder, CFD, manoeuvrability, energy efficiency

1 INTRODUCTION

The main operational task of a rudder in most ships is to act as a manoeuvre device, as well as an energy recovering device when interacting with the water flow leaving the propeller (the amount of energy which is recovered will depend on the form and thickness of the profile of the propeller, the aspect ratio, R_n , the spatial distribution of the velocity upstream and the turbulence of the flow "(Bertram, V. 2000)").

The flow is not stationary, mainly due to the rotation energy supplied by the propeller. The presence of the rudder also modifies the propulsion unit, blocking the exit section of the flow. The making of a numerical approach to this physical phenomenon by means of numerical simulations and the knowledge of the behaviour of the flow would imply the solution of an evolutionary problem on a moving mesh. This type of problems has high

computational costs and are not valid to be used in an industrial field. Some articles in the literature consulted demonstrate that they can be dealt with in a quite precise way by means of Reynolds Averaged Numerical Stationary Simulations so as to obtain integral values on the different regions of interest "(Caldas et al 2010)", "(Sánchez-Caja et al 2009)".

In this article, an analysis of the effect caused by the rudder on the unit propeller-nozzle for a 70m trawler is analyzed by means of numerical simulations. The study arises from the need the fishing fleet has at this crisis period, of having more energy-efficient ships, and takes into account interesting modifications which allow both a decrease in consumption and lower fuel expenses.

A general description of the cases, together with the numerical model is presented in Section 2. Calculations of the propeller-nozzle unit are presented in Section 3, and Section 4 describes the ones for the set propeller-nozzle-rudder. In both sections performance has been analyzed for open water. As the propulsion system works at the wake of a ship, the wake calculation of the ship studied at Section 5 will be used in Section 6 to show performance of it working behind the ship. Finally, conclusions are shown in Section 7.

2 GENERAL DESCRIPTION

The first aim of this article is to carry out a study on the effect the rudder exercises on the propulsive characteristics of ducted propeller units. A 70m trawler ship with a controllable pitch ducted propeller has been used.

2.1 Geometry and Physical Conditions

The general characteristics of the above mentioned ship are shown in Table 1.

Table 1. General Characteristics.

Lpp	69,2	m
B	12	m
T	4,75	m
V	11	kts
	4	kts
Engine Power	2700	HP
	1987,2	kW

It can be seen that two performance conditions are shown for the ship: first, a velocity of 11kts corresponding to free run, and then another one of 4kts corresponding to the trawling condition of the ship. Characteristics for the propeller are shown on Table 2.

Table 2. Propulsion. General Characteristics.

Propeller Diameter	2300	mm
Nozzle Diameter	2340	mm
Gap	1,7	%
P/D	1,032	-
EAR	0,756	-
Nozzle Length	1759	mm
Nozzle Length /Diameter	0,765	-

For behind simulations, the trawling performance conditions of the ship correspond to a pitch of 0,9 and an engine power of 85% MCR.

Taking into account that the purpose of the present article is to carry out a study on the effect the rudder geometry has on the propulsive characteristics, we define below the geometry of the original configuration of the rudders. As we can see in Figure 1, the initial configuration is made up of a pair of rudders off-centered the propeller shaft.

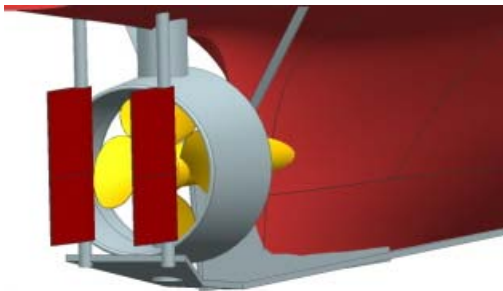


Figure 1. Propulsion. Initial Configuration.

Characteristics for these rudders are shown on Table 2.

Table 3. Original Rudders. Characteristics.

Rudder Chord	1500	mm
Rudder Height	2250	mm
Lateral Displacement	667	mm
Thickness	0,15*Chord	-

Trying to take into account the effect of different rudder configurations, two new arrays for the rudders have been generated (see Fig. 2). The first one is a three-rudder array with the same projected area as the in the original configuration. The second array is one single rudder with 65% of the projected area. General characteristics for these three arrays are summed up in Table 4.

Table 4. General characteristics of the three geometries.

Case Id.	Case A	Case B	Case C	
Number of Rudders	2	3	1	-
Height-a	2250	2250	-	mm
Height-b	-	2460	2460	mm
Chord	1500	971	1784	mm
Projected Area	6,75	6,75	4,39	m ²
%	-	100%	65%	-
Height/chord	1,50	2,32	1,26	-
Thickness/chord	0,15	0,15	0,15	-
Thickness	225,0	145,7	267,5	mm
Wetted Surface	13,9	14,3	9,0	m ²

2.2 Numerical Methods

The mathematical model used for the calculation of the numerical simulations is described by Reynolds Averaged Navier Stokes Equations (RANSE). We get the couple of the Reynolds shear stress tensor by means of a two-equation model named Two Layer Realizable K-Epsilon using an All y+ Law for the wall modelling. The problem is closed establishing the initial and boundary conditions on the physical and computational boundaries. A no-slip condition is imposed on the solid walls (velocity = 0; normal pressure gradients = 0). A condition of velocity is imposed upstream, whereas downstream, there is a pressure condition. Regarding the initial conditions two types were established: for the first simulations a condition of constant velocity over all the domain, equal to the inlet velocity. For the rest of the simulations previous solutions were used as initial conditions so as to accelerate convergence. The free surface has not been modelled, as Froude number is low enough to disregard the deformations on it (Fn=0,07 for 4kts), making both modelling and resolution easier.

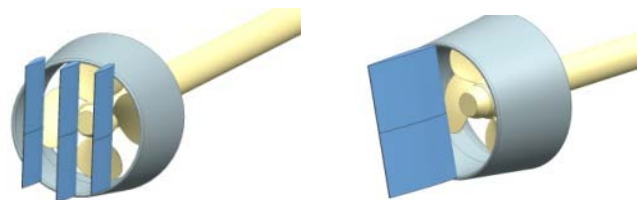


Figure 2. Case B (left) and Case C (right).

Commercial code StarCCM+ has been used for the numerical solutions of the equations. StarCCM+ solves RANSE equations in their integral form, by means of Finite Volumes methods. The numerical method uses second-order schemes both for viscous and convective terms. Velocities and pressures are solved in a segregated manner, and then coupled by means of the SIMPLE algorithm. The rotation of the propeller was modelled using a moving reference frame system. Regarding the mesh, calculations were made on a non-structured mesh of polyhedrons. In both cases, the y+ values range

between $y+=30$ and $y+=150$. The surface mesh in the propulsion unit can be seen in Figure 3.

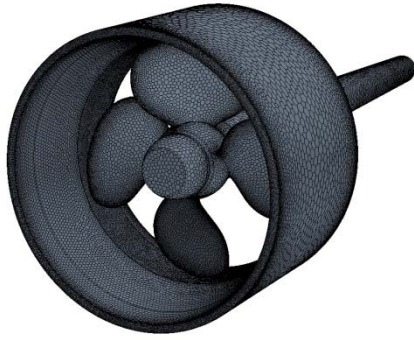


Figure 3. Propulsion. Spatial discretization.

Despite the geometry presents longitudinal symmetry, this symmetry cannot be applied as the rudders presence leads to instabilities by means of the introduction of physical asymmetry in the problem (i.e., it produces a flow block at the exit of the propeller).

2.2 Figures of Merit

The figures of merit used to establish the comparison among the three cases of study correspond to the following adimensional standard coefficients:

$$K_T = \frac{T}{\rho \cdot n^2 \cdot D^4} \quad K_Q = \frac{Q}{\rho \cdot n^2 \cdot D^5} \quad \eta = \frac{K_T \cdot J}{K_Q \cdot 2\pi}$$

$$K_{tp} = \frac{T_{Propeller}}{\rho \cdot n^2 \cdot D^4} \quad K_{tn} = \frac{T_{Nozzle}}{\rho \cdot n^2 \cdot D^4} \quad K_{tr} = \frac{T_{Rudder}}{\rho \cdot n^2 \cdot D^4}$$

where K_T = the thrust coefficient, K_Q = the torque coefficient, and η = the efficiency. The indexes p, n and r represents propeller, nozzle and rudder respectively.

3 OPEN WATER

As a first approximation, Open Water tests for the propeller with the nozzle have been carried out, at different advance ratios and at different pitch. Efficiency curves for the different working conditions of our propeller are shown in Figure 4.

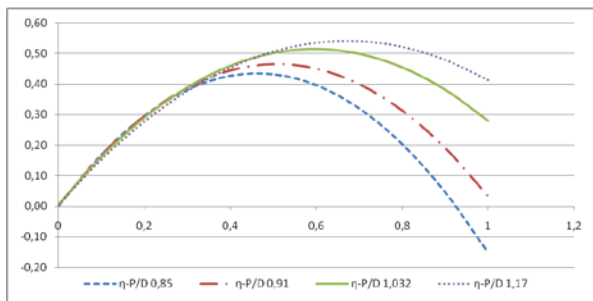


Figure 4. Efficiency curves for different pitch.

Thrust and torque coefficients calculated for different pitches of the propeller are shown in Figures 5 and 6 .

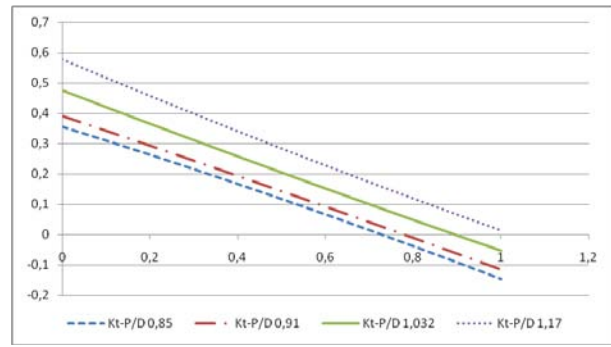


Figure 5. Curves for K_T at different pitch.

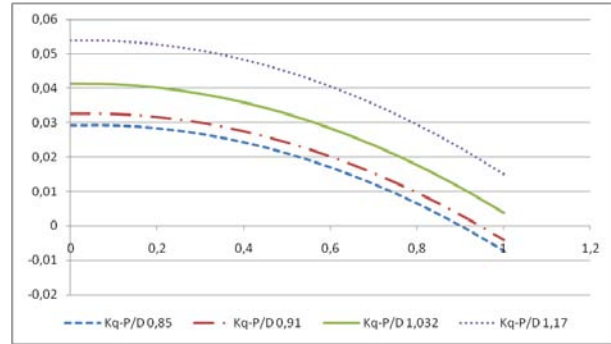


Figure 6. Curves for K_Q at different pitch.

The choice of boundary conditions, shape and size of the computational domain used is the same as the one described in "Caldas et al (2010)" as well as the validation of the boundary conditions for this type of ducted propellers.

4 OPEN WATER WITH RUDDER

Calculations using the three rudder configurations described on Section 2.1 have been carried out for a propeller P/D relation of 1,032. In Figure 7, we can see the evolution of K_{tr} , an adimensional representation of the longitudinal forces on the rudder surface for different advance ratios.

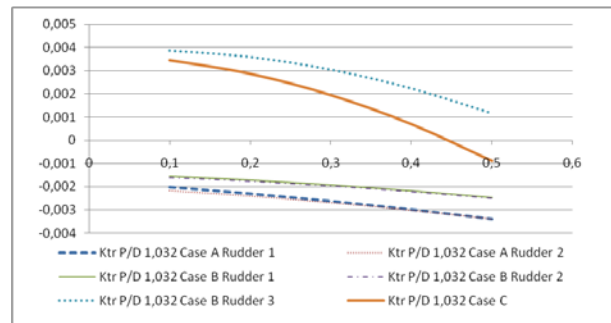


Figure 7. K_{tr} for the different rudders

In Figure 7 we can see that for original configuration (C-A) , both rudders induce to a negative force. In Case B, in which we have 3 rudders arrayed behind the propeller, only the central rudder recovers energy, taking place a longitudinal force in the forward direction of the ship. Regarding Case C, in which we have only one centred rudder, we also recover part of the rotational energy lost

by the propeller. In Figure 8, the variation of the thrust supplied by the propeller referred to the case where no rudder is present can be seen. It can be observed that, in all cases, the thrust supplied by the propeller is increased by placing a rudder downstream. The higher thrust increase is shown in the three-rudder case (C-B), followed by the case where one single centred rudder is present (C-C).

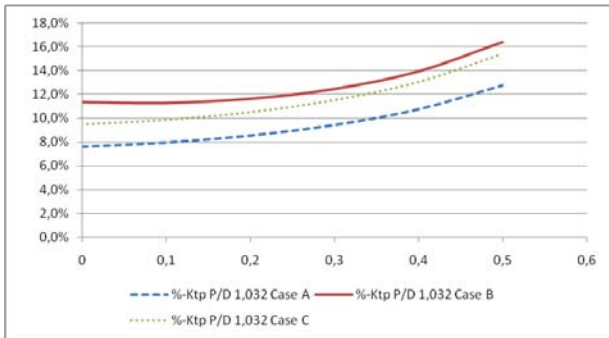


Figure 8. % K_{tp} referred to Open Water w-o rudder

The variation in the thrust supplied by the nozzle with regard to the no-rudder case is shown in Figure 9. We can see here how the effect on the nozzle is contrary to the one showed in the propeller, as there is a reduction of the load on the nozzle when the rudder is placed downstream. The higher thrust reduction is shown by Case B (three rudders). Here the thrust increase for the propeller was higher. Case A (2 rudders) shows the lower reduction. This can be related both to the rudders projected area on a perpendicular plane to the water flow and to the distribution of velocities downstream of the nozzle. The placing of a rudder downstream the nozzle causes a reduction of the area, so altering the characteristics of the flow around the nozzle. The case with the three rudders shows the highest reduction, followed by the 2-rudder and the single rudder cases.

The decrease in the area downstream produces a slight decrease in the velocity through the inner part of the nozzle and an increase of velocities outside. Locally, this induces an increase of the propeller load, and a decrease in the load of the nozzle. All this causes an increase of K_{tp} and a decrease of K_{tn} when we refer this values to the same case but with no rudders present.

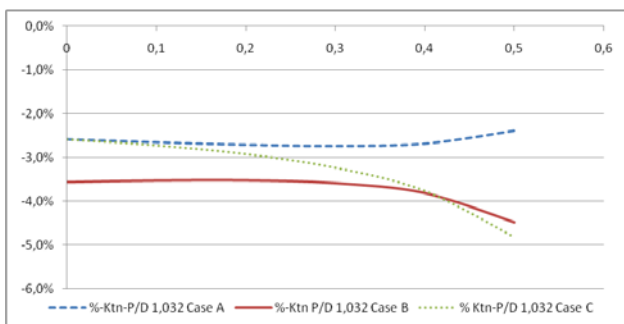


Figure 9. % K_{tn} referred to Open Water w-o rudder

The variation the total thrust with respect to Open Water without rudder is shown in Figure 10. The effects of the rudders, the propeller and the nozzle have been taken into

account. We can see that the worst of cases is the original of the ship (C-A), in which we have 2 off-centered rudders. Regarding thrust, the fact of introducing a central rudder improves the total K_T . Cases B and C are quite similar being Case C slightly higher.

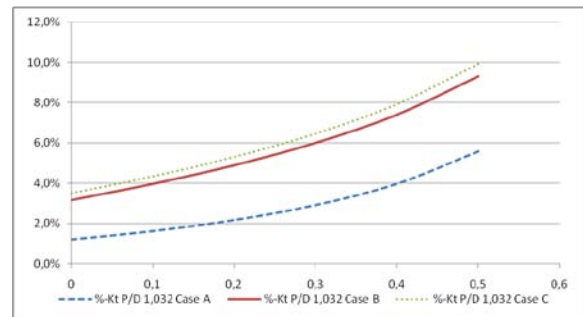


Figure 10. % K_T referred to Open Water w-o rudder

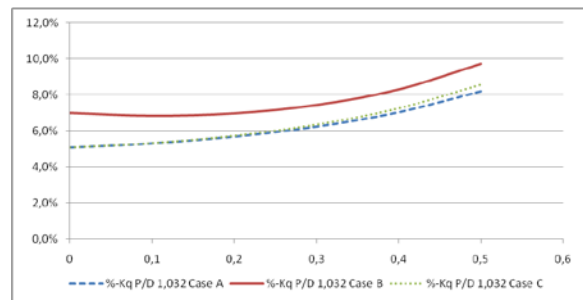


Figure 11. % K_Q referred to Open Water w-o rudder

In Figure 11 we see the torque variation with respect to Open Water without rudder for the three cases. The fact of introducing the rudders causes a torque increase: the higher one for the 3-rudder case. The original case (C-A) and the single rudder case (C-C) remain almost the same for all the range of advance ratio, slightly increasing when we increase J .

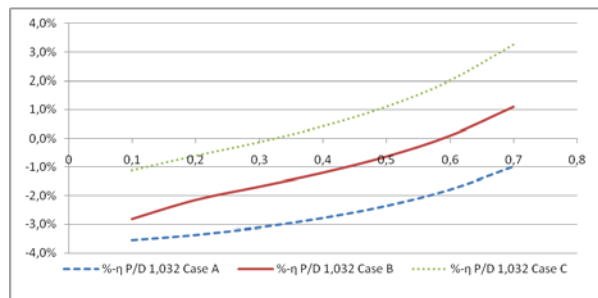


Figure 12. % Efficiency referred to Open Water w-o rudder

If we take into account the combined effect of thrust and torque, evaluated through efficiency (see Fig. 12), we see that Case C shows the highest efficiency, followed by Case B and the original one. In short it appears that, regarding the efficiency of the whole, the inclusion of the rudder aligned with the propeller shaft improves the energy efficiency of the propulsion system.

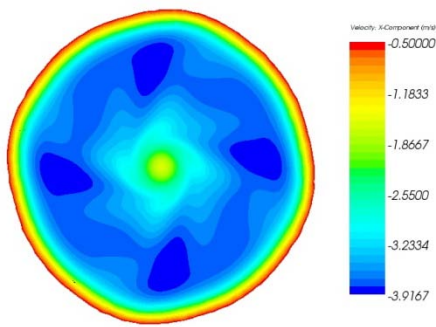


Figure 13. Velocities downstream the propeller $J=0,1$

The field of velocities over a perpendicular plane to the flow downstream the nozzle is shown in Figure 13. The field of velocities shows a radial dependence, the higher the radio, the higher field intensity (but in the near of the walls, due to the viscous effects). Besides, the shadow of the shaft in the centre and the areas of high velocity behind the propeller blades can be seen, though a bit displaced.

5 WAKE FIELD

Before studying the propulsion working in behind, a wake calculation has been carried out. In Figures 14 and 15 the results of such a calculation are shown (the angle is measured from the lower area of the propeller and counter-clockwise). As it can be seen in the figures, there are three areas with low velocities due to the shadows caused by geometry elements. There is a shadow in the lower part (angle 0) due to the keel. In the upper one there are two different shadows caused by the strut arms (angle 145) and to the upper side of the hull (angle 180). These two areas show different velocity values due to the distance between the geometrical elements and the propeller.

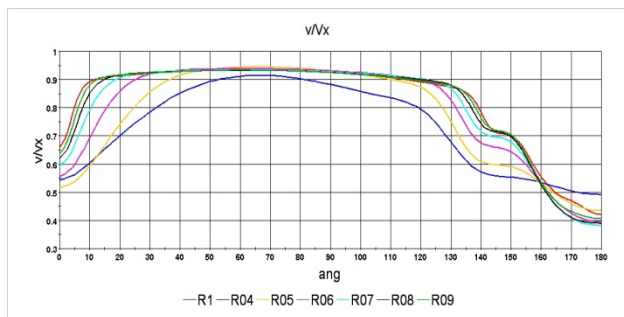


Figure 14. % Main circumferential wake

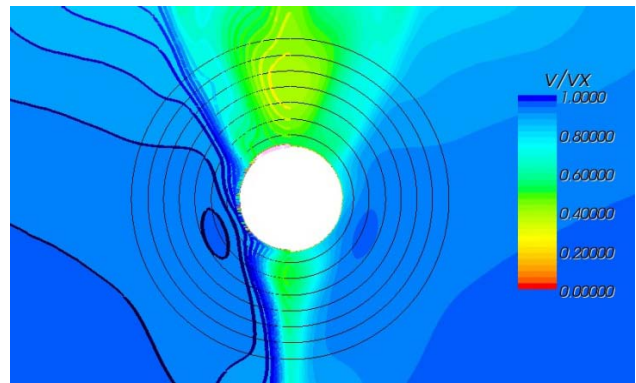


Figure 15. v/Vx in the propeller plane

6 BEHIND

Finally, in this section the results of the calculations of the propulsion working in the wake of the ship are shown. For the three cases studied, the suction coefficient (t) stays in constant values, being independent of the configuration of the rudders.

6.1 Trawling Condition

The comparison among the three cases is made on Case A (that is the reason why the percentage for Case A is of a 100% in all graphics). Figure 16 shows how the thrust of the rudders is opposed to the advance of the ship, both for Case A and Case B, whereas in the case of a single rudder the thrust coincides with the advance direction of the ship. The negative thrust in the off-centred rudder cases (Cases A and B) is due to the high flow velocity and also to the small angle of attack over the side rudders. The central rudder is the only one that can recover energy because the flow presents a slow velocity and so can give it energy.

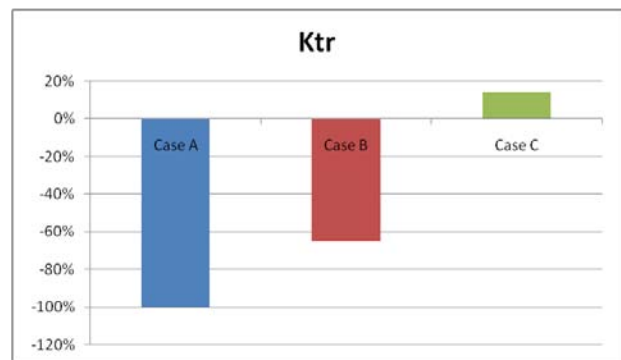


Figure 16. % K_{tr} referred to Case A

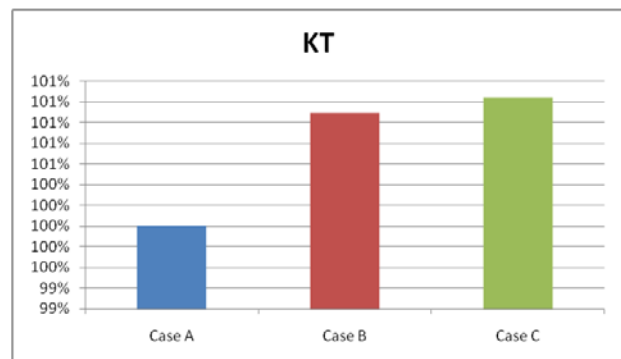


Figure 17. % K_T referred to Case A

Thrust coefficient of the whole propulsion system is shown in Figure 17. Figure 18 shows the torque coefficient. Also in Figure 18 it can be seen that the increase in the lock of the rudders causes a torque increase.

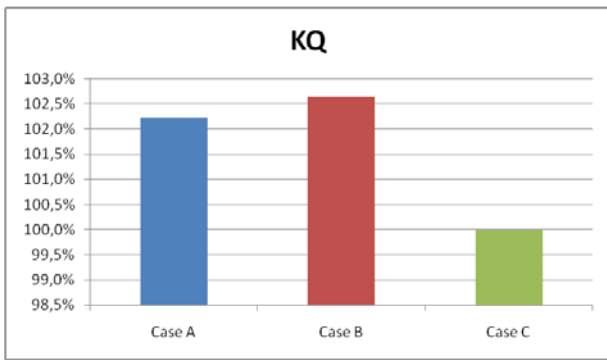


Figure 18. % K_Q referred to Case A

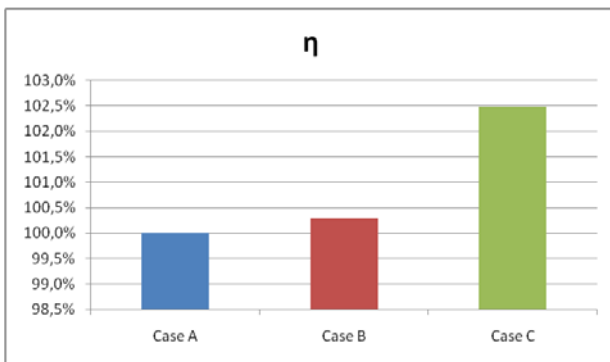


Figure 19. % Efficiency referred to Case A

With the presence of a single rudder – as it is shown in Figure 19- we can obtain an increase in efficiency of 2,5% with respect to the presence of rudders on the sides. This improvement is mainly due to both the torque decreasing at the propeller and the recovery of energy by the central rudder.

The influence of the rudders in the propulsion system during the trawling manoeuvre of the ship is also analyzed. For this, four angles are simulated (two at portside and two at starboard), being 30 degrees the highest angle of manoeuvre of the ship.

Figure 20 shows the longitudinal component of trawling force during the manoeuvre. As it can be seen, cases A and B show a worse behaviour than Case C. The behaviour of this force is directly related to the wetted surface of the rudders as, for bigger angles, a bigger wetted surface produces a higher trawling force when in manoeuvre.

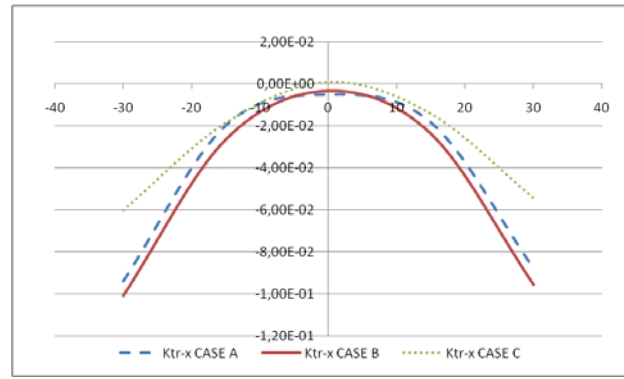


Figure 20. Longitudinal Force F_x

The side force in manoeuvre presents a lineal dependence with the turn angle for cases A and B. Case C presents a worse behaviour with the turn angle (Fig. 21). The behaviour of this force is related to the a projected area of the rudders. The values of side force –for case C- are approximately of a 60% of those for Cases A or B. This percentage is related to the projected area of the rudder, as the area of Case C is a 60% of the area for Cases A or B (see Table 4).

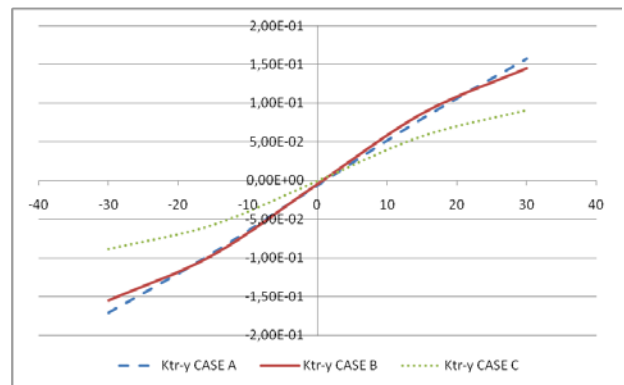


Figure 21. Side Force F_y

Figure 22 shows rudder stock torque. The smallest values correspond to Case C. Again, this is related to the projected area. Between Cases B and A we can see that the presence of the central rudder causes reductions in the rudder stock torque.

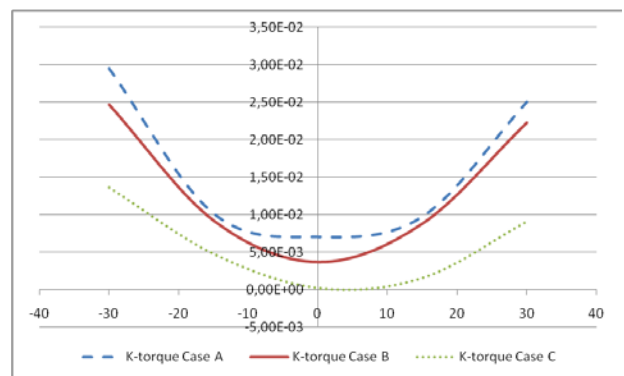


Figure 22. Rudder stock Torque

2.2 Free Run

Calculations in free run have also been carried out for the three cases of study, varying the pitch of the propeller. In this case, we have used the nominal pitch of the propeller, following measurements on board. Variations of K_T for the three configurations are shown in Figure 23. In this case, the tendency which has been observed in trawling condition is inverted (highest thrust is shown for Case A) basically due to 2 factors: the higher load of the nozzle in Case A (Fig. 24), and the fact that the configurations with a central rudder (Cases B and C) recover much less rotational energy due to the decrease of load at the propeller, with respect to the trawling case (Fig. 25). For torque, tendencies are the same as in the trawling case seen before. The highest value of K_Q is shown in Case B. The lowest value is shown in Case C. Again, the highest efficiency is for Case C.

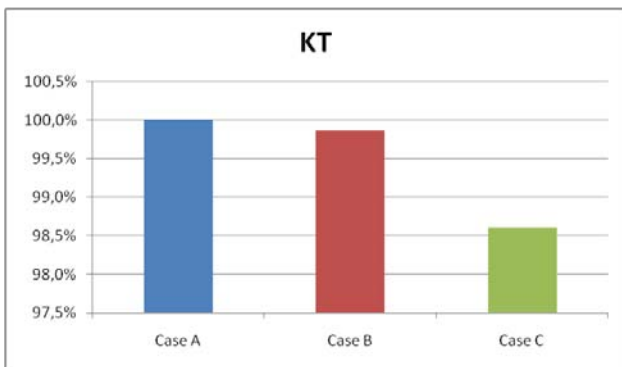


Figure 23. K_T Total

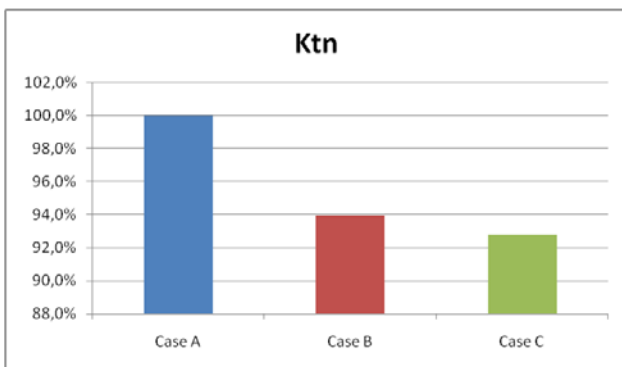


Figure 24. K_{tn} Nozzle

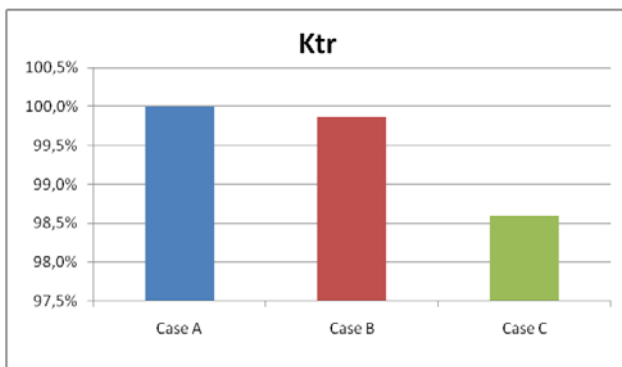


Figure 25. K_{tr} Rudder

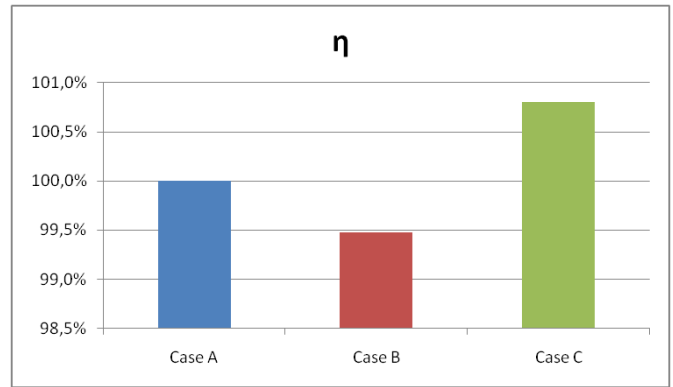


Figure 26. Efficiency

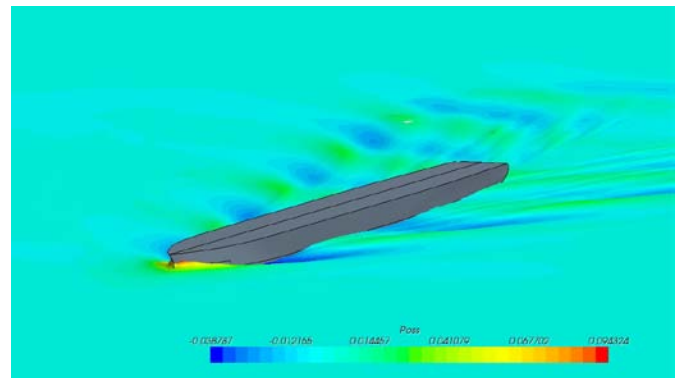


Figure 27. Wave map for 11 kts

7 CONCLUSIONS

This article presents a numerical study on the influence of rudders over the propulsion unit formed by propeller and nozzle for a 70 m trawler. The study consisted in analyzing the behaviour of three different rudder configurations: two off-centered rudders, three rudders and one rudder upon the ship propulsion in trawling condition, free run and manoeuvring.

The numerical analysis was made by means of the commercial Finite Volume code StarCCM+ employing a RANSE model. Free surface has not been considered in the model as Froude number is quite low. Finally note that the rotation of the propeller has been modelled using a moving reference frame system.

Trawling results, both for the Open Water condition and for the Behind one, clearly show that the best behaviour – from an efficiency point of view- is that shown in the case with a single central rudder, as the central rudder is the one which recovers a part of the rotational energy lost by the propeller as the velocity upstream is low.

The results obtained for trawling condition, both in Open Water as in Behind, prove the ability of the Open Water tests to determine in a qualitative way the tendencies of the different configurations. This conclusion has a special relevance for the design process as open water calculations will be less expensive in calculation time.

The configuration of the two off-centred rudders produces a higher side force, compared with that of a single central rudder when the ship during the manoeuvre during

trawling. Besides, if a central rudder is added to maintaining the projected area, an improvement in the trawling force and a better manoeuvrability characteristics will be achieved.

Regarding future studies, it is relevant to note the importance of studying how geometrical aspects of the rudder, as profile or aspect relations (relation between height and chord) as well as aspects related to its position from the propeller and the nozzle, can affect the operation of the propulsion unit of trawler ships, as these aspects condition on the whole the flow area downstream the nozzle and also the velocity field in the propeller.

REFERENCES

- Bertram, V (2000). Practical Ship Hydrodynamics. 2nd ed. Woburn: Butterworth-Heinemann
- Caldas, A., Meis, M., Sarasquete, A. (2010) CFD validation of different propeller ducts on Open Water condition. 13th Numerical Towing Tank Symposium, Germany.
- Ferziger, J.H. & Peric, M. (2002). Computational Methods for Fluid Dynamics. 3rd ed. Springer-Verlag Berlin Heidelberg.
- Reichel, M. (2009) Influence of rudder location on propulsive characteristics of a single screw container ship. First International Symposium on Marine Propulsors, Trondheim, Norway.
- Sánchez-Caja, A., Sipilä, T.P. & Pykkänen, J.V. (2009) Simulation of viscous flow around a ducted propeller with rudder using different RANS-based approaches. First International Symposium on Marine Propulsors, Trondheim, Norway.
- STAR CCM + User Guide (Version 4.0.6) (2009)